IEEE Access
Multidisciplinary | Rapid Review | Open Access Journal

Received May 21, 2021, accepted June 10, 2021, date of publication June 22, 2021, date of current version July 5, 2021.

Digital Object Identifier 10.1109/ACCESS.2021.3091544

Pseudo-Differential $(2 + \alpha)$-Order Butterworth Frequency Filter

ONDREJ SLADOK[1], JAROSLAV KOTON[1], (Senior Member, IEEE), DAVID KUBANEK[1], JAN DVORAK[1], AND COSTAS PSYCHALINOS[2], (Senior Member, IEEE)

[1]Department of Telecommunications, Brno University of Technology, 61600 Brno, Czech Republic
[2]Electronics Laboratory, Physics Department, University of Patras, 26504 Patras, Greece

Corresponding author: Jaroslav Koton (koton@vutbr.cz)

This work was supported by the Czech Science Foundation under Grant 19-24585S.

This work did not involve human subjects or animals in its research.

ABSTRACT This paper describes the design of analog pseudo-differential fractional frequency filter with the order of $(2 + \alpha)$, where $0 < \alpha < 1$. The filter operates in a mixed-transadmittance mode (voltage input, current output) and provides a low-pass frequency response according to Butterworth approximation. General formulas to determine the required transfer function coefficients for desired value of fractional order α are also introduced. The designed filter provides the beneficial features of fully-differential solutions but with a less complex circuit topology. It is canonical, i.e. it employs a minimum number of passive elements, whereas all are grounded, and current conveyors as active elements. The proposed structure offers high input impedance, high output impedance, and high common-mode rejection ratio. By simple modification, voltage response can also be obtained. The performance of the proposed frequency filter is verified both by simulations and experimental measurements proving the validity of theory and the advantageous features of the filter.

INDEX TERMS Current conveyor, fractional Butterworth transfer function, fractional-order filter, pseudo-differential filter.

I. INTRODUCTION

Within the last decades, there is a significantly rising attention being paid to fractional-order (FO) calculus due to its promising utilization in various research areas such as economy and finance [1]–[3], medical and health science [4]–[6], agriculture and food processing [7]–[10], automotive [11]–[13], and also in electrical engineering [14]–[43] to design, describe, model and/or control various systems and function blocks. Basically, the presence of fractional order (α) represents another degree of freedom to mathematically describe the behavior of a function block. This enables to provide characteristics in between integer-orders in comparison to classic (integer-order) circuits, which may become beneficial while more accurate signal generation and measurement, and/or system modeling and control is needed.

The associate editor coordinating the review of this manuscript and approving it for publication was Sai-Weng Sin.

In the discipline of electrical engineering and analog signal processing, FO frequency filters [14]–[28], oscillators [29]–[32], controllers [33]–[36], and FO element emulators and converters [37]–[43] are mostly discussed.

In case of analog circuit design and signal processing, the presence of the fractional-order element (FOE), having impedance with a non-integer power law dependence on the Laplace operator s, is generally necessary. However, FOEs are currently not readily available as discrete elements, as it is the case of classic resistors, capacitors and inductors, although a number of promising technologies is being investigated as has been recently summarized in [44]. Currently, there are generally two approaches to overcome the absence of discrete FOEs, both approximating the behavior of FOE in a specific frequency range and with required accuracy. The first approach approximates directly the term s^{α} being present in the transfer function by integer-order polynomial function. The originally FO transfer function turns into an integer-order one, which results in a more complex circuit counting more active and passive elements, see

TABLE 1. Comparison of relevant fractional-order filters.

Ref.	Filter order	ABB type:count	Passive el. type:count	FOE impl.	Transfer function	Mode	Sim/Meas
[14]	α	OTA:3	FC:2	Foster II	LP, HP, BP, BS, AP	voltage	yes/no
[15]	α	OTA:10	C:2	s^α approx.	LP	voltage	yes/no
[16]	α	OTA:10	C:2	s^α approx.	AP	current	yes/no
[17]	α	OTA:2	FC:1	Foster I	AP	current	yes/no
[18]	$1+\alpha$	opamp:2	R:10, C:3	s^α approx.	LP, HP	voltage	yes/yes
[19]	$1+\alpha$	CFOA:4	R:9/8, C:3/4	s^α approx.	LP, HP	voltage	yes/yes
[20]	$1+\alpha$	CFOA:8	R:16, C:3	s^α approx.	LP, HP, BP, BS	voltage	yes/no
[21]	$1+\alpha$	opamp:3	FC:1, R:6, C:1	Foster I	LP	voltage	yes/no
[22]	$1+\alpha$	CG-CCDDCC:4, VGA:1	FC:1, R:2, C:1	Foster I	LP, HP, BP, BS, AP	current	yes/no
[23]	$\alpha+\beta$	DVCC:1	FC:1, FL:1, R:1	Foster I	LP	voltage	yes/no
[24]	$\alpha+\beta+\gamma$	opamp:2	FC:3, R:6	Foster I	LP	voltage	yes/yes
[27]	$5+\alpha$	opamp:10	C:7, R22	s^α approx.	LP	voltage	yes/yes
[28]	$1+\alpha$, $2+\alpha$, $3+\alpha$, $1+\alpha+\beta$, $2+\alpha+\beta$, $\alpha+\beta$, $\alpha+\beta+\gamma$, $1+\alpha+\beta+\gamma$ $\alpha+\beta+\gamma+\delta$	OTA:4, IOGC-CA:1	FC:1–4, C:0–4	Foster I	LP	voltage	yes/no
proposed	$2+\alpha$	DDCC:1, DVCC:2, CCII:1	FC:1, C:2, R:4/6	Foster II	LP	mixed, voltage	yes/yes

List of previously unexplained abbreviations used in this table:
CFOA: Current Feedback Operational Amplifier, CG-CCDDCC: controlled gain current-controlled differential difference current conveyor, VGA: Variable Gain Amplifier, IOGC-CA: individual output gain controlled current amplifier
C: capacitor, R: resistor, FC: capacitive FOE, FL: inductive FOE
LP: low-pass, HP: high-pass, BP: band-pass, BS: band-stop, AP: all-pass

e.g., [15], [16]. The second approach approximates primarily the required FOE, most commonly by a RC ladder network, such as Foster I, Foster II, Cauer I and Cauer II [45]. The advantage of this second approach is that the complexity of the final circuit solution increases only by the count of the resistors and capacitors that are used to approximate the FOE, see e.g., [14], [24]. Additionally, once FOEs become readily available as solid-state, it will be only necessary to replace the RC ladder network by the specific FOE. This is not the case of the FO circuits being designed using the first approach (i.e. designed by direct approximation of s^α), whereas these circuit solutions will become basically obsolete. An overview of FO frequency filters designed by both above described approaches can be found in Table 1. The different types of active building blocks (ABBs) are used to design fractional filters of α- or $(1+\alpha)$-order, primarily operational transconductance amplifiers (OTAs) and operational amplifiers (opamps). Fractional-order solutions of higher-order filters are rare as presented in [25]–[27], and are based on Butterworth approximation. However, the issue of circuits described in [25]–[27] is that both partial transfer functions are determined by using Butterworth approximation. Thus, the resulted $(N+\alpha)$-order transfer function does not correspond to Butterworth approximation anymore, see e.g., [25] and [26] featuring at the pole-frequency the decrease in magnitude of 6 dB and not the commonly expected 3 dB, or showing significant peaking for some values of α [27]. Design of FO higher-order filters is also discussed in [28], where the proposed filter offers a wide variety of possible order combinations and to design up to $(3+\alpha)$-order filter. Although the experimental results are presented, the obtained frequency responses do not follow any common approximation type. Therefore, in this paper we primarily provide general formulas to determine $(2+\alpha)$-order transfer function coefficients for Butterworth approximation.

Next to FO filter design, in this paper we also contribute to the design of pseudo-differential frequency filters. Compared to "true" fully-differential circuits, whose circuit topology is also fully differential (e.g., [46]–[51]), the pseudo-differential structures as presented e.g., in [52]–[62] also provide the advantages of higher ability to reject the common-mode noise signals, suppress power supply noise, or feature higher dynamic range together with reduced harmonic distortion of the processed signal. However, pseudo-differential filters keep the simplicity of the circuit solutions being comparable to single-ended filters [63]–[65]. The solutions of pseudo-differential filters from [52]–[62] use different types of ABBs, primarily from the family of current conveyors (CCs). Table 2 summarizes the key features of such pseudo-differential filters. Basically, the proposed circuit solution may be used for the design of 3rd-order filter, where the fractional capacitor (FC) is replaced by classic capacitor. However, within further circuit analyses, simulations and experimental measurements, its FO version is assumed.

In this paper, we merge the two research topics and contribute both to pseudo-differential and FO frequency filter design. The filter operates in mixed (transadmittance) mode and provides a low-pass $(2+\alpha)$-order response according to Butterworth approximation. The current conveyors are advantageously used as active elements to maintain both high input and output (infinite in ideal case) impedance. By a simple modification, the filter can operate also in voltage mode. The performance of the proposed filter is verified both by simulation and experimental measurements to show its proper behavior.

The paper is organized as follows: Section II provides the theory on pseudo-differential filters, while the description

TABLE 2. Comparison of relevant pseudo-differential filters.

Ref.	Filter order	ABB type:count	R/C:count	All grounded	Transfer function	Mode	Sim/Meas	CMRR
[52]	1	DC-DVCC:2	4/2	no	LP, HP, AP	current	yes/no	no
[53]	1	DDCC:1	3/1	no	AP	voltage	yes/no	no
[54]	1	DV-DXCCII:1	3/2	no	AP	voltage	yes/no	no
[55]	2	FDCCII:3	6/4	yes	BP	mixed	yes/no	no
[56]	2	FDCCII: 1	5/4	no	BP	voltage	yes/no	no
[57]	2	CDCC:7	8/2	yes	LP, HP, BP	current	yes/no	no
[58]	2	DDCC:2, CCII:1	2/2	yes	BS	voltage	yes/yes	yes
[59]	2	DDCC:2, DVCC:2	3/2	yes	LP, HP, BP, BS, AP	voltage	yes/yes	yes
[60]	3	DDCC:4	3/3	yes	LP	voltage	yes/no	no
[61]	4	DDCC:4, CCII: 2	4/4	yes	LP	voltage	yes/yes	yes
[62]	5	CDCC:10	15/5	yes	LP	current	yes/no	no
proposed	3 2 + α	DDCC:1, DVCC:2, CCII:1	4(6)/3 4(6)/2 + FC:1	yes	LP	mixed, voltage	no/no yes/yes	no yes

List of previously unexplained abbreviations used in this table:
CCII: Second Generation CC, DDCC: Differential Difference CC, DVCC: Differential Voltage CC, CDCC: Current Differencing CC, DC-DVCC: Digitally-Controlled DVCC, DV-DXCCII: Differential Voltage Dual-X CC, FDCCII: Fully differential CC

of fractional $(2+\alpha)$-order transfer function approximated according to Butterworth is presented in Section III. The proposed filter is described in Section IV, where both the transadmittance- and voltage-mode transfer functions are given. Designing two prototypes of FOEs ($\alpha = 0.3$ and $\alpha = 0.6$) the simulation and experimental measurement results are presented in Section V, where not only the magnitude and phase frequency responses, but also the low total harmonic distortion (THD) and the common-mode rejection ratio (CMRR) were determined. Section VI concludes the paper.

II. THEORY ON PSEUDO-DIFFERENTIAL FILTERS

Dealing generally with any differential circuit, the following notation for differential input voltage (v_{1d}), common-mode input voltage (v_{1c}) and differential output voltage (v_{2d}) is assumed [66]:

$$v_{1d} = v_{1+} - v_{1-}, \quad v_{1c} = \frac{v_{1+} + v_{1-}}{2}, \quad v_{2d} = v_{2+} - v_{2-}, \quad (1)$$

whereas similarly a set of relations valid for current-mode differential circuits is specified:

$$i_{1d} = i_{1+} - i_{1-}, \quad i_{1c} = \frac{i_{1+} + i_{1-}}{2}, \quad i_{2d} = i_{2+} - i_{2-}. \quad (2)$$

The differential input signal v_{1d} (or i_{1d}) is simply the difference between the two input signals v_{1+} and v_{1-} (or i_{1+} and i_{1-}), whereas the common-mode input signal v_{1c} (or i_{1c}) is the average of the two input signals.

In the view of (1), the differential-output voltage v_{2d} is then defined as:

$$v_{2d} = A_{dm} v_{1d} + A_{cm} v_{1c}, \quad (3)$$

where A_{dm} and A_{cm} are the differential and the common-mode voltage gains, respectively. The capability of the differential circuit to reject the common-mode signal in voltage-mode signal processing is determined by the common-mode rejection ratio (CMRR) defined as [66]:

$$CMRR = 20 \log \left(\frac{A_{dm}}{A_{cm}} \right). \quad (4)$$

Similarly to (3) and using (2), the differential output current i_{2d} can be defined as:

$$i_{2d} = B_{dm} i_{1d} + B_{cm} i_{1c}, \quad (5)$$

where B_{dm} and B_{cm} are the differential and the common-mode current gains, respectively, and similarly to (4) the common-mode rejection ratio of a current-mode differential circuit can be determined:

$$CMRR = 20 \log \left(\frac{B_{dm}}{B_{cm}} \right). \quad (6)$$

From the viewpoint of general mathematical description of differential circuits using (1)–(6), it is evident that the inner circuit topology is never taken into account. Hence, dealing with differential circuits, it is not necessary to absolutely assume the circuit topology to be differential also. As a result, the ''pseudo'' fully-differential (or simply pseudo-differential) filters can be designed being specific with rather single-ended circuit topology but still providing differential input and output. Compared to ''true'' fully-differential filters, the main benefit of pseudo-differential filters is their significantly reduced complexity in the count of required active and passive elements of the final structure, which is usually twice smaller. At the same time, they keep the positive properties of ''true'' fully-differential filters, such as high common-mode rejection ratio and low harmonic distortion.

III. (2 + α) BUTTERWORTH APPROXIMATION

For the purpose of $(2+\alpha)$-order frequency filter design, the following general low-pass transfer function is assumed as:

$$H^{\mathrm{LP}}_{2+\alpha}(s) = \frac{1}{s^{2+\alpha} k_1 + s^2 k_2 + s k_3 + k_4}, \quad (7)$$

where $0 < \alpha < 1$, and k_1, k_2, k_3, and k_4, are the transfer function coefficients that were determined using an optimization algorithm to match the target Butterworth fractional low-pass magnitude response.

The relation for the magnitude of the target Butterworth FO low-pass transfer function generalized to fractional order

$(2+\alpha)$ can be written as follows:

$$|H_{2+\alpha}^{\mathrm{LP-T}}(\omega)| = \frac{1}{\sqrt{1+\omega^{2(2+\alpha)}}}, \tag{8}$$

that provides unity pass-band gain, magnitude of -3 dB at cut-off angular frequency 1 rad/s, and stop-band roll-off $-20(2+\alpha)$ dB/dec.

Using numerical optimization algorithm, the coefficients k_1, k_2, k_3, and k_4 from (7) were found such that the maximum absolute error between magnitude in dB of (7) and (8) is minimized. For this purpose, the MATLAB function *fminsearch* was used with the following fitness function:

$$f = \max_i \left| 20\log\left|H_{2+\alpha}^{\mathrm{LP}}(x,\omega_i)\right| - 20\log\left|H_{2+\alpha}^{\mathrm{LP-T}}(\omega_i)\right| \right|, \tag{9}$$

where x is the sought vector of the coefficients k_1, k_2, k_3, and k_4. Each search used 100 frequency points logarithmically spaced in the wide frequency range from $\omega_1 = 0.01$ rad/s to $\omega_{100} = 100$ rad/s to cover both pass- and stop-band of (8). The individual runs of *fminsearch* function were performed for the fractional component α decreasing from 0.99 to 0.01 with a linear step 0.01.

As a result, the transfer function coefficients k_1, k_2, k_3, and k_4 that yield the lowest error according to (9) for specific value of fractional order α are shown in Fig. 1. For better convenience, to determine the transfer function coefficients k_1, k_2, k_3, and k_4 in (7) according to Butterworth approximation for specific values of fractional order α, the following interpolation matrix can be used:

$$\begin{bmatrix} k_1 \\ k_2 \\ k_3 \\ k_4 \end{bmatrix} = \begin{bmatrix} 0.357 & 0.138 & -0.026 & 0.519 \\ 0.630 & 1.051 & -0.507 & 0.820 \\ 1.415 & 0.542 & -0.108 & 0.151 \\ 1.000 & -0.004 & -0.001 & 0.005 \end{bmatrix} \begin{bmatrix} 1 \\ \alpha \\ \alpha^2 \\ \alpha^3 \end{bmatrix}, \tag{10}$$

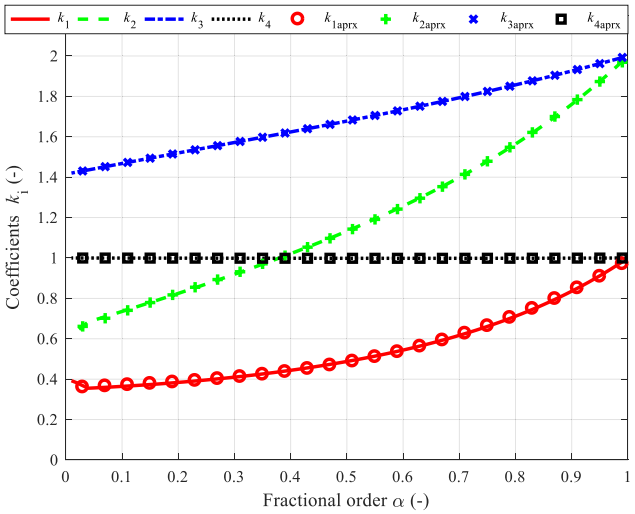

FIGURE 1. Coefficients k_1, k_2, k_3, and k_4 to approximate fractional Butterworth magnitude response using (7) reached by optimization process.

and in Fig. 1 shown as k_{1aprx}, k_{2aprx}, k_{3aprx}, and k_{4aprx} are compared to coefficients values of k_1, k_2, k_3, and k_4 determined using the fitness function (9).

To prove sufficient accuracy while determining the transfer function coefficients using the interpolation matrix (10), the relative error between coefficients k_1, k_2, k_3, and k_4 determined using the MATLAB *fminsearch* function and the interpolated coefficients using (10) is shown in Fig. 2. It can be seen that for $0.03 < \alpha < 1$ the relative error is always below 2%.

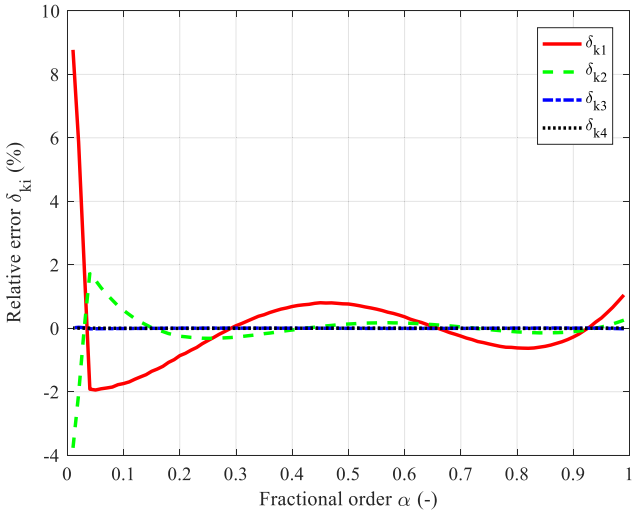

FIGURE 2. Relative error between coefficients k_1, k_2, k_3, and k_4 found using the MATLAB *fminsearch* function and determined by (10).

Before the coefficients k_1, k_2, k_3, and k_4 determined by (10) can be utilized to compute the values of the capacitors and resistors in the filter structure, the frequency shifting to the cut-off frequency ω_0 should be carried out, as the target function (8) has the -3 dB cut-off frequency 1 rad/s, which is not practical. Thus the transfer function coefficients should be modified by dividing them by the respective power of ω_0 as follows:

$$H_{2+\alpha,\omega_0}^{LP}(s) = \frac{1}{s^{2+\alpha}\frac{k_1}{\omega_0^{2+\alpha}} + s^2\frac{k_2}{\omega_0^2} + s\frac{k_3}{\omega_0} + k_4}. \tag{11}$$

IV. PROPOSED PSEUDO-DIFFERENTIAL FRACTIONAL-ORDER FILTER

To design the frequency filter, the current conveyors DVCC (Differential Voltage Current Conveyor), DDCC (Differential Difference Current Conveyor) and CCII (Second Generation Current Conveyor) as active elements have been advantageously used, whose schematic symbols are shown in Fig. 3.

Both DVCC and DDCC are based on CCII, only have additional input voltage terminals Y, and therefore, for all types it holds that the Y terminal i_Y currents are zero. Also for all active elements and their Z+/− terminal currents it holds:

$$i_{Z+} = i_X, \quad i_{Z-} = -i_X. \tag{12}$$

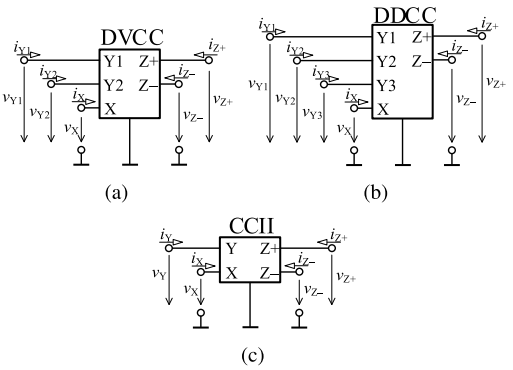

FIGURE 3. Schematic symbols of (a) DVCC, (b) DDCC, (c) CCII.

The only significant difference between the assumed current conveyor types is the formula specifying the voltage at X terminal:

$$\left.\begin{aligned} &\text{for DVCC}: v_X = v_{Y1} - v_{Y2} \\ &\text{for DDCC}: v_X = v_{Y1} - v_{Y2} + v_{Y3} \\ &\text{for CCII}: \quad v_X = v_Y \end{aligned}\right\} \tag{13}$$

Using the current conveyors, the proposed pseudo-differential filter suitable to provide a $(2 + \alpha)$-order low-pass frequency response operating in transadmittance- or voltage-mode is shown in Fig. 4(a) and Fig. 4(b), respectively. The principal structure of the filter is based on inverse follow the leader feedback (IFLF). The $DDCC_1$, $DVCC_2$ and $DVCC_3$ together with the corresponding passive elements operate as integrators. Taking the advantage of the $DDCC_1$ and its voltage terminals, the differential input voltage v_{1d} is directly applied to the Y1 and Y2 terminals and hence high input impedance of the proposed filters is ensured. The $CCII_4$ primarily serves as voltage-to-current converter and provides the differential current output (Fig. 4(a)).

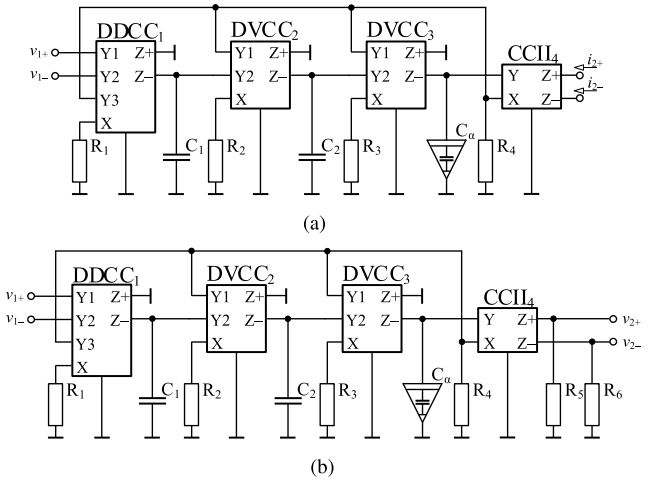

FIGURE 4. Proposed pseudo-differential $(2 + \alpha)$-order frequency filter operating in: (a) transadmittance-mode, (b) voltage-mode.

Following the general mathematical description of differential filters as discussed in Section II, the output currents i_{2+} and i_{2-} of the filter from Fig. 4(a) can be determined as:

$$i_{2+}(s) = \frac{1}{R_4}\frac{1}{s^{2+\alpha}u_1 + s^2u_2 + su_3 + 1}v_{1d} + 0v_{1c}, \tag{14}$$

$$i_{2-}(s) = -\frac{1}{R_4}\frac{1}{s^{2+\alpha}u_1 + s^2u_2 + su_3 + 1}v_{1d} + 0v_{1c}, \tag{15}$$

where $u_1 = C_1C_2C_\alpha R_1R_2R_3$, $u_2 = C_1C_2R_1R_2$, and $u_3 = C_1R_1$, whereas C_α is the pseudo-capacitance of the fractional capacitor and α is its fractional order.

From (14) and (15), the differential transadmittance gain is defined as:

$$G_{dm} = \frac{2}{R_4}\frac{1}{s^{2+\alpha}u_1 + s^2u_2 + su_3 + 1}, \tag{16}$$

and the common-mode transamittance gain G_{cm} is zero.

As shown in Fig. 4(b), adding extra two resistors (R_5 and R_6) the proposed filter may be operated in voltage-mode. The output voltages v_{2+} and v_{2-} are then determined as:

$$v_{2+}(s) = -\frac{R_5}{R_4}\frac{1}{s^{2+\alpha}u_1 + s^2u_2 + su_3 + 1}v_{1d} + 0v_{1c}, \tag{17}$$

$$v_{2-}(s) = \frac{R_6}{R_4}\frac{1}{s^{2+\alpha}u_1 + s^2u_2 + su_3 + 1}v_{1d} + 0v_{1c}, \tag{18}$$

and for the differential voltage gain it holds:

$$A_{dm} = -\frac{R_5 + R_6}{R_4}\frac{1}{s^{2+\alpha}u_1 + s^2u_2 + su_3 + 1}, \tag{19}$$

whereas the common-mode voltage gain A_{cm} is zero and the common-mode rejection ratio CMRR is infinite, in theory.

V. SIMULATIONS AND EXPERIMENTAL MEASUREMENTS

The properties of the proposed pseudo-differential FO frequency filter from Fig. 4(b), i.e. operating in voltage-mode, were verified by simulations and mainly also by experimental measurements. Both for simulations and experiments the Universal Current Conveyor UCC-N1B integrated circuit [67] was used to obtain the required types of active elements.

A. FRACTIONAL-ORDER ELEMENT DESIGN

Due to commercial unavailability of fractional capacitors in general, the required C_α was approximated using the 7th-order Foster II RC network as shown in Fig. 5. Using [45], the values of the resistors and capacitors of the Foster II network were determined, whereas to validate the performance of the proposed filter, two different FOEs were chosen:

- $\alpha = 0.3$, $C_\alpha = 7.038\ \mu\text{Fs}^{-0.7}$,
- $\alpha = 0.6$, $C_\alpha = 0.158\ \mu\text{Fs}^{-0.4}$,

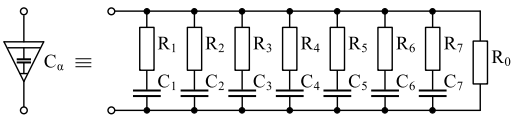

FIGURE 5. 7th-order Foster II RC network.

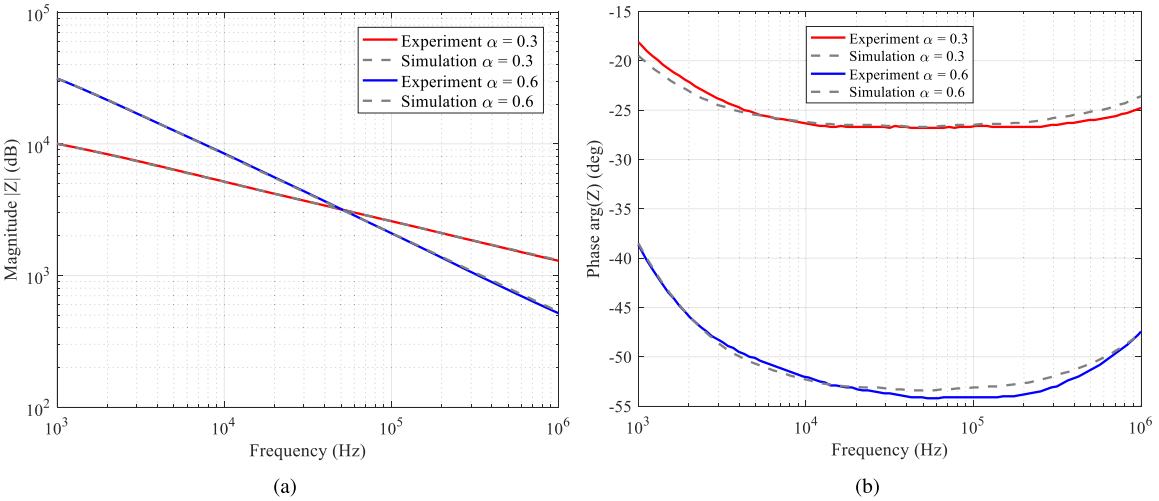

FIGURE 6. Simulation and experimental measurement results of the approximated FOEs for two values of α: (a) impedance magnitude, (b) impedance phase.

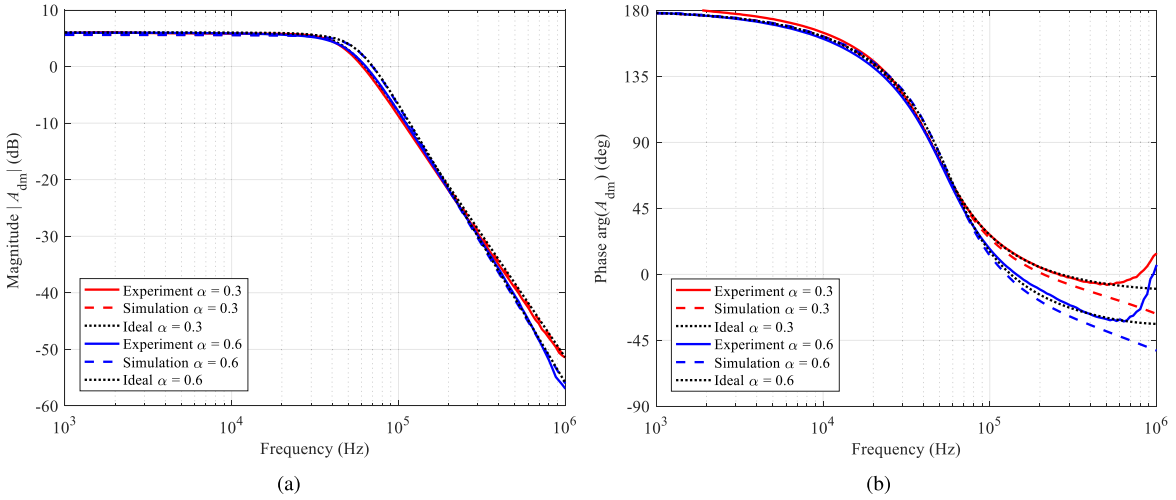

FIGURE 7. Simulation and experimental measurement results of the filter: (a) magnitude responses, (b) phase responses.

with central frequency (f_C) of 50 kHz and approximation range from 5 kHz to 500 kHz. Both assumed FOEs feature the impedance module of 3184 Ω at f_C. The calculated values of the resistors and capacitors used to approximate the FOEs using the Foster II RC network from Fig. 5 are summarized in Table 3, whereas for simulations and experimental measurements, the values for resistors and capacitors were selected from the E24 and E12 series, respectively.

The impedance module and phase shift of the two approximated FOEs obtained by measurements and compared to the simulation results are shown in Fig. 6. From Fig. 6(a), for $\alpha = 0.3$ the value of module of the approximated FOEs at central frequency 50 kHz is 3176 Ω, whereas for $\alpha = 0.6$ the impedance module is and 3198 Ω, which is very close to the expected value of 3184 Ω for ideal FOEs. The results in Fig. 6(b) show the phase shift validate proper approximation in the specified frequency range, i.e. from 5 kHz to 500 kHz.

B. PERFORMANCE ANALYSIS OF THE FILTER

For the selected values of α, using (10) the coefficients k_1, k_2, k_3 and k_4 of the general transfer function (7) were determined. Choosing the values of capacitors $C_1 = C_2 = 1$ nF and the filter pole-frequency $f_0 = 50$ kHz and using (19), the values of resistors R_1, R_2 and R_3 were determined as 5.00 kΩ, 1.86 kΩ and 1.41 kΩ, respectively, and are the same for both FOEs as their module at the pole-frequency is also the same. The values of the resistors R_4, R_5, and R_6 were selected to be 1 kΩ.

The magnitude and phase responses of the proposed filter obtained both by simulations and experimental measurements are displayed in Fig. 7(a) and Fig. 7(b), respectively. From the characteristics, it can be clearly seen that both simulation and

TABLE 3. Values of resistors and capacitors in 7th-order Foster II RC network.

	$\alpha = 0.3$	$\alpha = 0.6$
R_0	12.7 kΩ	50.5 kΩ
R_1	2.12 kΩ	290 Ω
R_2	3.83 kΩ	1.14 kΩ
R_3	5.87 kΩ	2.78 kΩ
R_4	8.82 kΩ	6.28 kΩ
R_5	13.2 kΩ	14.1 kΩ
R_6	20.0 kΩ	32.3 kΩ
R_7	33.3 kΩ	87.7 kΩ
C_1	24.0 pF	143 pF
C_2	49.2 pF	135 pF
C_3	119 pF	207 pF
C_4	295 pF	342 pF
C_5	735 pF	569 pF
C_6	1.80 nF	922 pF
C_7	4.04 nF	1.30 nF

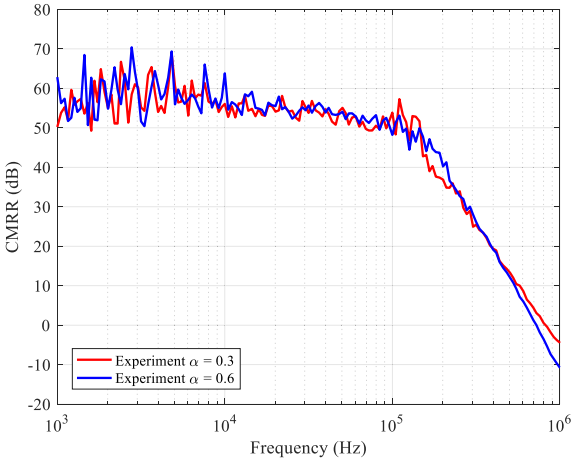

FIGURE 8. Measured CMRR of the pseudo-differential filter.

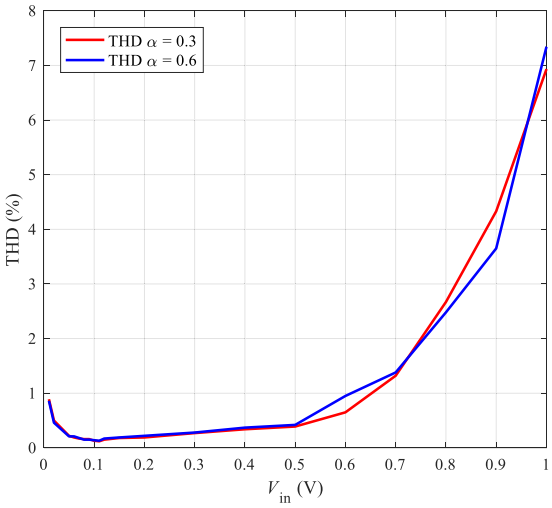

FIGURE 9. Measured THD of the pseudo-differential filter.

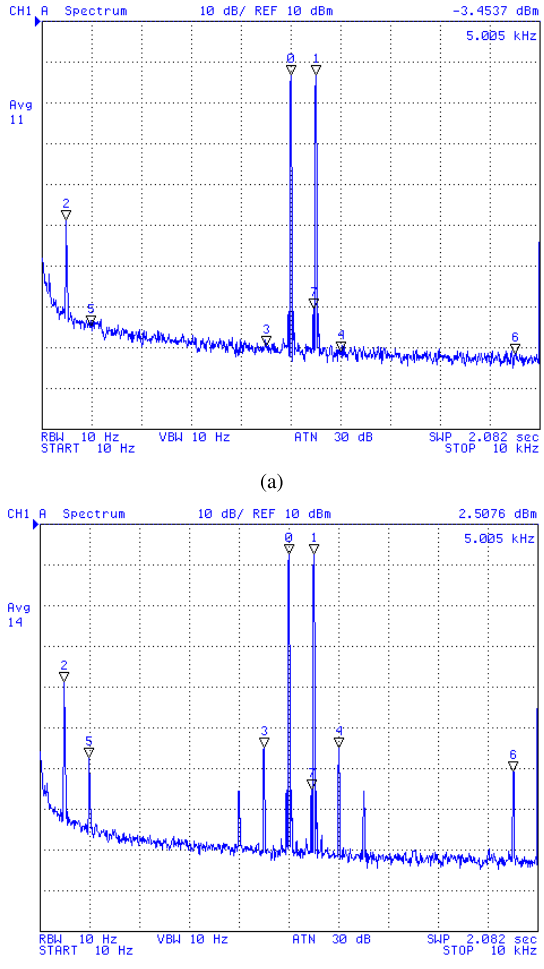

FIGURE 10. Measured spectum at the output of the filter for (a) V_{in} = 200 mVpp, (b) V_{in} = 400 mVpp.

experimental measurements follow theoretical presumptions very well. For experimental measurements, the deviation at frequencies above approx. 600 kHz is attributed to parasitic properties and frequency limitations of the active element UCC-N1B [67]. The UCC-N1B is an integrated circuit that was designed as laboratory sample in cooperation with ON Semiconductor company. The chip includes one Universal Current Conveyor (UCC), used to obtain the DDCC and DVCCs, and one CCII+/–.

In addition to the measured magnitude and phase response characteristics, the ability of the pseudo-differential filter to suppress the common-mode signal, the CMRR was experimentally measured. The results are shown in Fig. 8. For both cases of used FOE, the value of CMRR is above 50 dB in the pass band of the filter. The decrease in CMRR above approx. 200 kHz is due to the actual behavior of the UCC-N1B and the mismatch of the voltage gains β_1 and β_2 between terminals Y1 and X, and terminals Y2 and X of the active element as we investigated earlier in [58].

The total harmonic distortion (THD) was also evaluated by means of experimental measurements. The reached results are shown in Fig. 9. Similarly, to measuring CMMR, also here the THD is close for both values of fractional order α and is below 2% for the amplitude of the input signal up to 0.7 V at frequency 1 kHz.

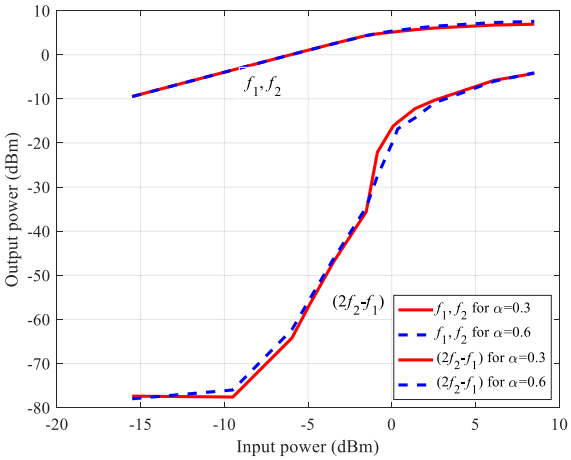

FIGURE 11. Relationship between the fundamental (f_1, f_2) and 3rd-order IMD ($2f_2 - f_1$) on input signal level.

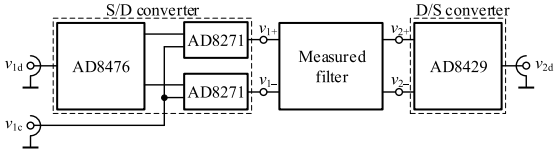

FIGURE 12. Block diagram of the experimental measurement setup.

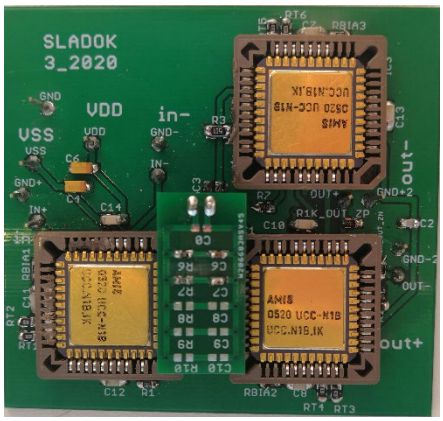

FIGURE 13. The PCB prototype of the pseudo-differential voltage-mode filter from Fig. 4(b).

Finally, the intermodulation distortion (IMD) was determined, whereas using 81150A generator, two fundamental tones f_1 and f_2 with frequency of 5 kHz and 5.5 kHz were applied. In Fig. 10 the spectrums at the output of the filter are shown for two different input voltages. From Fig. 10(b) the 3rd IMD harmonic suppression is 47.5 dB for $V_{\text{in}} = 400$ mVpp. The relationship between the fundamental (f_1, f_2) and 3rd-order IMD $(2f_2 - f_1)$ on input signal level is shown in Fig. 11. From Fig. 11 the -1 dB gain compression point is at 0.73 dBm of the input power.

Performing the experimental measurements to reach the results as presented above, primarily the network analyser Agilent 4395A was used. To obtain the differential input signal and be too able to measure the differential output response, single-to-differential (S/D) and differential-to-single (D/S) converters had to be added and were implemented using AD8476 [68] and AD8429 [69] integrated circuits respectively. For the sake of evaluating also CMRR of the proposed pseudo-differential filter, the AD8271 [70] was used to apply common-mode signal at the input of the filter. The total block connection for experimental measurements is shown in Fig. 12. For sake of completeness the PCB prototype of the measured voltage-mode pseudo-differential filter is also shown in Fig. 13.

VI. CONCLUSION

This article contributes to the design of FO filters, whereas the mathematical calculus enabling to determine the $(2+\alpha)$-order transfer function coefficients according to Butterworth approximation for arbitrary α was presented. Besides, new circuit solution of the pseudo-differential filter was also proposed and used to prove and support the theory both of the designing pseudo-differential and fractional-order filters. The structure operates in mixed-mode (transadmittance) and thanks to current conveyors, used as active elements, it features high input and output impedance. It was shown that simple modification enables to operate the filter in voltage-mode. Both simulation and experimental measurements show proper behavior of the filter in magnitude and phase and moreover prove high CMRR and dynamic range keeping total harmonic distortion low.

REFERENCES

[1] H. U. Rehman, M. Darus, and J. Salah, "A note on Caputo's derivative operator interpretation in economy," *J. Appl. Math.*, vol. 2018, pp. 1–7, Oct. 2018, doi: 10.1155/2018/1260240.

[2] V. E. Tarasov, "On history of mathematical economics: Application of fractional calculus," *Mathematics*, vol. 7, no. 9, p. 509, 2019, doi: 10.3390/math7060509.

[3] P. Roul and V. M. K. P. Goura, "A high order numerical method and its convergence for time-fractional fourth order partial differential equations," *Appl. Math. Comput.*, vol. 366, Feb. 2019, Art. no. 124727, doi: 10.1016/j.amc.2019.124727.

[4] C. Ionescu, A. Lopes, D. Copot, J. A. T. Machado, and J. H. T. Bates, "The role of fractional calculus in modeling biological phenomena: A review," *Commun. Nonlinear Sci. Numer. Simul.*, vol. 51, pp. 141–159, Oct. 2017, doi: 10.1016/j.cnsns.2017.04.001.

[5] D. Kumar and J. Singh, *Fractional Calculus in Medical and Health Science*. Boca Raton, FL, USA: CRC Press, 2020, doi: 10.1201/9780429340567.

[6] J. M. Munoz-Paceco, C. Posadas-Castillo, and E. Zambrano-Serrano, "The effect of a non-local fractional operator in an asymmetrical glucose-insulin regulatory system: Analysis, synchronization and electronic implementation," *Symmetry*, vol. 12, no. 9, pp. 1–22, 2020, doi: 10.3390/sym12091395.

[7] N. Su, *Fractional Calculus for Hydrology, Soil Science and Geomechanics: An Introduction to Applications*. Boca Raton, FL, USA: CRC Press, 2020, doi: 10.1201/9781351032421.

[8] A. M. Lopes, J. A. T. Machado, and E. Ramalho, "On the fractional-order modeling of wine," *Eur. Food Res. Technol.*, vol. 243, no. 6, pp. 921–929, Jun. 2017, doi: 10.1007/s00217-016-2806-x.

[9] G. D. S. Matias, C. A. Bissaro, L. M. D. M. Jorge, and D. F. Rossoni, "The fractional calculus in studies on drying: A new kinetic semi-empirical model for drying," *J. Food Process. Eng.*, vol. 42, no. 1, Feb. 2019, Art. no. e12955, doi: 10.1111/jfpe.12955.

[10] G. D. S. Matias, F. H. Lermen, K. Y. Gonçalves, L. M. D. M. Jorge, J. L. D. Ribeiro, and T. M. Coelho, "A semi-empirical model for mass transfer in carbohydrate polymers: A case of native cassava starch hydration kinetic in hot water media," *Starch*, vol. 72, nos. 11–12, Nov. 2020, Art. no. 1900308, doi: 10.1002/star.201900308.

[11] I. Tejado, V. Milanés, J. Villagrá, and B. M. Vinagre, "Fractional network-based control for vehicle speed adaptation via vehicle-to-infrastructure communications," *IEEE Trans. Control Syst. Technol.*, vol. 21, no. 3, pp. 780–790, May 2013, doi: 10.1109/TCST.2012.2195494.

[12] C. Flores, V. Milanés, and F. Nashashibi, "Using fractional calculus for cooperative car-following control," in *Proc. IEEE 19th Int. Conf. Intell. Transp. Syst. (ITSC)*, Rio de Janeiro, Brazil, Nov. 2016, pp. 907–912, doi: 10.1109/ITSC.2016.7795663.

[13] G. A. Munoz-Hernandez, G. Mino-Aguilar, J. F. Guerrero-Castellanos, and E. Peralta-Sanchez, "Fractional order PI-based control applied to the traction system of an electric vehicle (EV)," *Appl. Sci.*, vol. 10, no. 1, pp. 2–23, 2020, doi: 10.3390/app10010364.

[14] G. Singh, Garima, and P. Kumar, "Fractional order capacitors based filters using three OTAs," in *Proc. 6th Int. Conf. Control, Autom. Robot. (ICCAR)*, Singapore, Apr. 2020, pp. 638–643. [Online]. Available: https://ieeexplore.ieee.org/document/9108100, doi: 10.1109/ICCAR49639.2020.9108100.

[15] M. R. Dar, N. A. Kant, F. A. Khanday, and C. Psychalinos, "Fractional-order filter design for ultra-low frequency applications," in *Proc. IEEE Int. Conf. Recent Trends Electron., Inf. Commun. Technol. (RTEICT)*, Bangalore, India, May 2016, pp. 1727–1730, doi: 10.1109/RTEICT.2016.7808129.

[16] M. V. Bhat, S. S. Bhat, and D. V. Kamath, "G_m-C current mode fractional all pass filter of order α ($0 < \alpha < 1$)," in *Proc. 3rd Int. Conf. Electron. Commun. Aerosp. Technol. (ICECA)*, Coimbatore, India, Jun. 2019, pp. 240–245, doi: 10.1109/ICECA.2019.8822183.

[17] D. V. Kamath, S. Navya, and N. Soubhagyaseetha, "Fractional order OTA-C current-mode all-pass filter," in *Proc. 2nd Int. Conf. Inventive Commun. Comput. Technol. (ICICCT)*, Coimbatore, India, Apr. 2018, pp. 383–387, doi: 10.1109/ICICCT.2018.8473097.

[18] T. J. Freeborn, B. Maundy, and A. Elwakil, "Towards the realization of fractional step filters," in *Proc. IEEE Int. Symp. Circuits Syst.*, Paris, France, May 2010, pp. 1037–1040, doi: 10.1109/ISCAS.2010.5537360.

[19] R. Verma, N. Pandey, and R. Pandey, "CFOA based low pass and high pass fractional step filter realizations," *AEU, Int. J. Electron. Commun.*, vol. 99, pp. 161–176, Feb. 2019, doi: 10.1016/j.aeue.2018.11.032.

[20] G. Tsirimokou, R. Sotner, J. Jerabek, J. Koton, and C. Psychalinos, "Programmable analog array of fractional-order filters with CFOAs," in *Proc. 40th Int. Conf. Telecommun. Signal Process. (TSP)*, Barcelona, Spain, Jul. 2017, pp. 706–709, doi: 10.1109/TSP.2017.8076079.

[21] A. Soni and M. Gupta, "Design of fractional order Butterworth filter using genetic algorithm," in *Proc. 2nd IEEE Int. Conf. Power Electron., Intell. Control Energy Syst. (ICPEICES)*, Delhi, India, Oct. 2018, pp. 1052–1055, doi: 10.1109/ICPEICES.2018.8897371.

[22] L. Langhammer, R. Sotner, J. Dvorak, J. Jerabek, and P. A. Ushakov, "Novel electronically reconfigurable filter and its fractional-order counterpart," in *Proc. 26th IEEE Int. Conf. Electron., Circuits Syst. (ICECS)*, Genoa, Italy, Nov. 2019, pp. 538–541, doi: 10.1109/ICECS46596.2019.8965165.

[23] S. K. Mishra, M. Gupta, and D. K. Upadhyay, "Active realization of fractional order Butterworth lowpass filter using DVCC," *J. King Saud Univ., Eng. Sci.*, vol. 32, no. 2, pp. 158–165, Feb. 2020, doi: 10.1016/j.jksues.2018.11.005.

[24] A. M. Hassanein, A. Soltan, L. A. Said, A. H. Madian, and A. G. Radwan, "Analysis and design of fractional-order low-pass filter with three elements of independent orders," in *Proc. Novel Intell. Lead. Emerg. Sci. Conf. (NILES)*, Giza, Egypt, Oct. 2019, pp. 218–221, doi: 10.1109/NILES.2019.8909312.

[25] T. J. Freeborn, "Comparison of $(1 + \alpha)$ fractional-order transfer functions to approximate lowpass Butterworth magnitude responses," *Circuits, Syst., Signal Process.*, vol. 35, pp. 1983–2002, Jun. 2016, doi: 10.1007/s00034-015-0226-y.

[26] T. J. B. Freeborn, B. Maundy, and A. S. Elwakil, "Field programmable analogue array implementation of fractional step filters," *IET Circuits Devices Syst.*, vol. 4, no. 6, pp. 514–524, Nov. 2010, doi: 10.1049/iet-cds.2010.0141.

[27] B. Maundy, A. S. Elwakil, and T. J. Freeborn, "On the practical realization of higher-order filters with fractional stepping," *Signal Process.*, vol. 91, no. 3, pp. 484–494, Mar. 2011, doi: 10.1016/j.sigpro.2010.06.018.

[28] L. Langhammer, J. Dvorak, R. Sotner, J. Jerabek, and P. Bertsias, "Reconnection–less reconfigurable low–pass filtering topology suitable for higher–order fractional–order design," *J. Adv. Res.*, vol. 25, pp. 257–274, Sep. 2020, doi: 10.1016/j.jare.2020.06.022.

[29] L. A. Said, A. G. Radwan, A. H. Madian, and A. M. Soliman, "Two-port two impedances fractional order oscillators," *Microelectron. J.*, vol. 55, pp. 40–52, Sep. 2016, doi: 10.1016/j.mejo.2016.06.003.

[30] O. Elwy, L. A. Said, A. H. Madian, and A. G. Radwan, "All possible topologies of the fractional-order Wien oscillator family using different approximation techniques," *Circuits, Syst., Signal Process.*, vol. 38, no. 9, pp. 3931–3951, Feb. 2019, doi: 10.1007/s00034-019-01057-6.

[31] A. S. Elwakil, A. Agambayev, A. Allagui, and K. N. Salama, "Experimental demonstration of fractional-order oscillators of orders 2.6 and 2.7," *Chaos, Solitons Fractals*, vol. 96, pp. 160–164, Mar. 2017, doi: 10.1016/j.chaos.2017.01.017.

[32] L. A. Said, O. Elwy, A. H. Madian, A. G. Radwan, and A. M. Soliman, "Stability analysis of fractional-order Colpitts oscillators," *Anal. Integr. Circuits Signal Process.*, vol. 101, no. 2, pp. 267–279, Jul. 2019, doi: 10.1007/s10470-019-01501-2.

[33] S. A. David, R. V. D. Sousa, C. A. Valentim, R. A. Tabile, and J. A. T. Machado, "Fractional PID controller in an active image stabilization system for mitigating vibration effects in agricultural tractors," *Comput. Electron. Agricult.*, vol. 131, pp. 1–9, Dec. 2016, doi: 10.1016/j.compag.2016.11.001.

[34] P. Lino, G. Maione, S. Stasi, F. Padula, and A. Visioli, "Synthesis of fractional-order PI controllers and fractional-order filters for industrial electrical drives," *IEEE/CAA J. Autom. Sinica*, vol. 4, no. 1, pp. 58–69, Jan. 2017, doi: 10.1109/JAS.2017.7510325.

[35] A. Tepljakov, *Fractional-Order Modeling and Control of Dynamic Systems*. Cham, Switzerland: Springer, 2017, doi: 10.1007/978-3-319-52950-9.

[36] M. Dulău, A. Gligor, and T.-M. Dulău, "Fractional order controllers versus integer order controllers," *Procedia Eng.*, vol. 181, pp. 538–545, Jan. 2017, doi: 10.1016/j.proeng.2017.02.431.

[37] G. Tsirimokou, C. Psychalinos, A. S. Elwakil, and K. N. Salama, "Electronically tunable fully integrated fractional-order resonator," *IEEE Trans. Circuits Syst. II, Exp. Briefs*, vol. 65, no. 2, pp. 166–170, Feb. 2018, doi: 10.1109/TCSII.2017.2684710.

[38] R. Sotner, L. Polak, J. Jerabek, and J. Petrzela, "Simple two operational transconductance amplifiers-based electronically controllable bilinear two port for fractional-order synthesis," *Electron. Lett.*, vol. 54, no. 20, pp. 1164–1166, Oct. 2018, doi: 10.1049/el.2018.5575.

[39] S. Kapoulea, C. Psychalinos, A. S. Elwakil, and A. G. Radwan, "One-terminal electronically controlled fractional-order capacitor and inductor emulator," *AEU, Int. J. Electron. Commun.*, vol. 103, pp. 32–45, May 2019, doi: 10.1016/j.aeue.2019.03.002.

[40] A. Adhikary, P. Sen, S. Sen, and K. Biswas, "Design and performance study of dynamic fractors in any of the four quadrants," *Circuits, Syst., Signal Process.*, vol. 35, no. 6, pp. 1909–1932, Jun. 2016, doi: 10.1007/s00034-015-0213-3.

[41] M. C. Tripathy, D. Mondal, K. Biswas, and S. Sen, "Experimental studies on realization of fractional inductors and fractional-order bandpass filters," *Int. J. Circuit Theory Appl.*, vol. 43, no. 9, pp. 1183–1196, Sep. 2015, doi: 10.1002/cta.2004.

[42] A. Adhikary, S. Choudhary, and S. Sen, "Optimal design for realizing a grounded fractional order inductor using GIC," *IEEE Trans. Circuits Syst. I, Reg. Papers*, vol. 65, no. 8, pp. 2411–2421, Aug. 2018, doi: 10.1109/TCSI.2017.2787464.

[43] J. Koton, D. Kubanek, J. Dvorak, and N. Herencsar, "On systematic design of fractional-order element series," *Sensors*, vol. 21, no. 4, pp. 1–23, 2021, doi: 10.3390/s21041203.

[44] Z. M. Shah, M. Y. Kathjoo, F. A. Khanday, K. Biswas, and C. Psychalinos, "A survey of single and multi-component fractional-order elements (FOEs) and their applications," *Microelectron. J.*, vol. 84, pp. 9–25, Feb. 2019, doi: 10.1016/j.mejo.2018.12.010.

[45] G. Tsirimokou, "A systematic procedure for deriving RC networks of fractional-order elements emulators using MATLAB," *AEU, Int. J. Electron. Commun.*, vol. 78, pp. 7–14, Aug. 2017, doi: 10.1016/j.aeue.2017.05.003.

[46] M. I. Masud, A. K. B. A'ain, and I. A. Khan, "Reconfigurable CNTFET based fully differential first order multifunctional filter," in *Proc. Int. Conf. Multimedia, Signal Process. Commun. Technol. (IMPACT)*, Aligarh, India, Nov. 2017, pp. 55–59, doi: 10.1109/MSPCT.2017.8363973.

[47] E. M. Spinelli, M. A. Mayosky, and R. J. Mantz, "Independent common-mode and differential-mode design of fully differential analog filters," *IEEE Trans. Circuits Syst. II, Exp. Briefs*, vol. 53, no. 7, pp. 572–576, Jul. 2006, doi: 10.1109/TCSII.2006.875311.

[48] N. Herencsar, J. Jerabek, J. Koton, K. Vrba, S. Minaei, and I. C. Göknar, "Pole frequency and pass-band gain tunable novel fully-differential current-mode all-pass filter," in *Proc. IEEE Int. Symp. Circuits Syst. (ISCAS)*, Lisbon, Portugal, May 2015, pp. 2668–2671, doi: 10.1109/ISCAS.2015.7169235.

[49] P. Beg, I. A. Khan, S. Maheshwari, and M. A. Siddiqi, "Digitally programmable fully differential filter," *Radioengineering*, vol. 20, no. 4, pp. 917–925, 2011.

[50] L. Langhammer, R. Sotner, J. Dvorak, J. Jerabek, and M. Zapletal, "Fully-differential universal frequency filter with dual-parameter control of the pole frequency and quality factor," in *Proc. IEEE Int. Symp. Circuits Syst. (ISCAS)*, Florence, Italy, May 2018, pp. 1–5, doi: 10.1109/ISCAS.2018.8351005.

[51] J. Dvorak, J. Jerabek, L. Langhammer, S. Kapoulea, and C. Psychalinos, "Design of fully-differential frequency filter with fractional-order elements," in *Proc. 41st Int. Conf. Telecommun. Signal Process. (TSP)*, Athens, Greece, Jul. 2018, pp. 1–7, doi: 10.1109/TSP.2018.8441259.

[52] M. S. Ansari and G. S. Soni, "Digitally-programmable fully-differential current-mode first-order LP, HP and AP filter sections," in *Proc. Int. Conf. Signal Propag. Comput. Technol. (ICSPCT)*, Ajmer, India, Jul. 2014, pp. 524–528, doi: 10.1109/ICSPCT.2014.6884963.

[53] J.-W. Horng, C.-M. Wu, and N. Herencsar, "Fully differential first-order allpass filters using a DDCC," *Indian J. Eng. Mater. Sci.*, vol. 21, pp. 345–350, Aug. 2014.

[54] P. Beg and M. S. Ansari, "Fully-differential first-order all-pass filters using CMOS DV-DXCCII," in *Proc. Int. Conf. Multimedia, Signal Process. Commun. Technol. (IMPACT)*, Aligarh, India, Nov. 2017, pp. 267–270, doi: 10.1109/MSPCT.2017.8364018.

[55] A. A. El-Adawy, A. M. Soliman, and H. O. Elwan, "A novel fully differential current conveyor and applications for analog VLSI," *IEEE Trans. Circuits Syst. II, Analog Digit. Signal Process.*, vol. 47, no. 4, pp. 306–313, Apr. 2000, doi: 10.1109/82.839666.

[56] S. A. Mahmoud, "Fully differential CMOS CCII based on differential difference transconductor," *Anal. Integr. Circuits Signal Process.*, vol. 50, no. 3, pp. 195–203, Feb. 2007, doi: 10.1007/s10470-007-9026-z.

[57] A. K. Singh and P. Kumar, "A novel fully differential current mode universal filter," in *Proc. IEEE 57th Int. Midwest Symp. Circuits Syst. (MWSCAS)*, College Station, TX, USA, Aug. 2014, pp. 579–582, doi: 10.1109/MWSCAS.2014.6908481.

[58] J. Koton, N. Herencsar, O. Sladok, and J.-W. Horng, "Pseudo-differential second-order band-reject filter using current conveyors," *AEU, Int. J. Electron. Commun.*, vol. 70, no. 6, pp. 814–821, Jun. 2016, doi: 10.1016/j.aeue.2016.03.009.

[59] O. Sladok, J. Koton, and N. Herencsar, "Universal pseudo-differential filter using DDCC and DVCCs," *Elektronika ir Elektrotechnika*, vol. 23, no. 6, pp. 46–52, Dec. 2017, doi: 10.5755/j01.eie.23.6.19694.

[60] O. Sladok, "Pseudo-differential high-order frequency filter," in *Proc. 25th Conf. STUDENT EEICT*, Brno, Czech Republic, 2019, pp. 764–768.

[61] O. Sladok, M. Milota, J. Koton, and N. Herencsar, "Systematic design of pseudo-differential frequency filter," in *Proc. 11th Int. Congr. Ultra Modern Telecommun. Control Syst. Workshops (ICUMT)*, Dublin, Ireland, Oct. 2019, pp. 1–6, doi: 10.1109/ICUMT48472.2019.8971000.

[62] A. K. Singh, P. Kumar, and R. Senani, "Fully-differential current-mode higher order filters using all grounded passive elements," *AEU, Int. J. Electron. Commun.*, vol. 97, pp. 102–109, Dec. 2018, doi: 10.1016/j.aeue.2018.10.009.

[63] S. Maheshwari, J. Mohan, and D. S. Chauhan, "Novel cascadable all-pass/notch filters using a single FDCCII and grounded capacitors," *Circuits, Syst., Signal Process.*, vol. 30, no. 3, pp. 643–654, Jun. 2011, doi: 10.1007/s00034-010-9238-9.

[64] W.-K. Chen, *Passive, Active, and Digital Filters*, 2nd ed. Boca Raton, FL, USA: CRC Press, 2009, doi: 10.1201/9781315219141.

[65] P. Bruschi, N. Nizza, F. Pieri, M. Schipani, and D. Cardisciani, "A fully integrated single-ended 1.5–15-Hz low-pass filter with linear tuning law," *IEEE J. Solid-State Circuits*, vol. 42, no. 7, pp. 1522–1528, Jul. 2007, doi: 10.1109/JSSC.2007.899081.

[66] U. Tietze, C. Schenk, and E. Gamm, *Electronic Circuits: Handbook for Design and Application*, Berlin, Germany: Springer-Verlag, 2008, doi: 10.1007/978-3-540-78655-9.

[67] Brno University of Technology and ON Semiconductor. (2012). *Datasheet UCC-N1B 0520: Universal Current Conveyor (UCC) and Second-Generation Current Conveyor (CCII+/−), Rev. 1*. [Online]. Available: https://www.utko.fekt.vut.cz/sites/default/files/inline-files/ucc-n1b_rev1.pdf

[68] *Datasheet AD 8476: Low Power, Unity Gain, Fully Differential Amplifier and ADC Driver*, Rev. B, Analog Devices, Norwood, MA, USA, 2012.

[69] *Datasheet AD 8429: 1 nV/$\sqrt{\text{Hz}}$ Low Noise Instrumentation Amplifier*, Analog Devices, Norwood, MA, USA, 2011.

[70] *Datasheet AD 8271: Programmable Gain Precision Difference Amplifier*, Analog Devices, Norwood, MA, USA, 2009.

ONDREJ SLADOK was born in Pelhrimov, Czech Republic, in 1991. He received the B.Sc. degree in teleinformatics from the Brno University of Technology (BUT), Czech Republic, in 2014, and the M.Sc. degree in communications and informatics from the Faculty of Electrical Engineering and Communication, BUT, in 2016, where he is currently pursuing the Ph.D. degree in teleinformatics.

Since 2017, he has been with the Department of Telecommunications, Faculty of Electronic Engineering and Communication, BUT, as a Research Assistant. From 2017 to 2020, he worked with InfoTel Company, which provides complex telecommunications services related to the construction and maintenance of telecommunications networks for the domestic and foreign market (Vodafone Czech Republic, T-Mobile Czech Republic, Orange SK, Deutsche Telekom, and Telefonica Deutschland). He is the author or coauthor of 11 articles. His research interests include development pseudo-differential frequency filters, fractional-order circuits and systems, further analog circuit theory, and signal processing.

JAROSLAV KOTON (Senior Member, IEEE) was born in Hustopece, Czech Republic, in 1981. He received the M.S. degree in electronics and communication and the Ph.D. degree in teleinformatics from the Brno University of Technology (BUT), Czech Republic, in 2005.

Since 2005, he has been with the Department of Telecommunications, Faculty of Electronic Engineering and Communication, BUT, where he was a Research Assistant, from 2013 to 2019, became an Associate Professor, and a Full Professor. From 2014 to 2018, he was the Vice-Head with the Department of Telecommunications. He currently serves as the Vice-Dean of research and Ph.D. studies with the Faculty of Electronic Engineering and Communication. He is currently the Head of the Analog Group dealing with the development and testing of electronic circuits, elements, and prototypes. He is the author or coauthor of more than 130 articles, and more than ten innovations. His research interests include analog circuit theory, signal processing, system modeling using fractional calculus, impedance spectroscopy, and active element design.

DAVID KUBANEK was born in Prerov, Czech Republic, in 1978. He received the M.S. degree in electronics and communication and the Ph.D. degree in teleinformatics from the Brno University of Technology (BUT), Czech Republic, in 2002 and 2006, respectively.

Since 2006, he has been an Assistant Professor with the Department of Telecommunications, Faculty of Electronic Engineering and Communication, BUT. He has authored 25 articles published in SCI-E peer-reviewed journals and about 35 papers in conference proceedings. He has participated on numerous research projects supported by the Czech Science Foundation. His research interests include design and analysis of analog electronic circuits, devices and elements, frequency filters, oscillators, impedance converters, non-linear circuits, and fractional-order circuits and systems. Since 2019, he has been serving as an Editorial Board Member of the *Fractal and Fractional* journal.

JAN DVORAK was born in Boskovice, Czech Republic, in 1990. He received the M.Sc. and Ph.D. degrees from the Brno University of Technology, Czech Republic, in 2015 and 2020, respectively.

He is currently with the Department of Telecommunications, Faculty of Electrical Engineering and Communication, Brno University of Technology. In 2019, he collaborated with the CEITEC Research Center, Masaryk University, as a Developer of hardware for sterilization of biological materials. He is the author or coauthor of 50 journal and/or conference papers. His research interests include analogue circuits, their design and verification of their features by simulations, and experimental measurements. His work is focused on fractional-order and integer-order circuits in the current mode, electronically tunable and reconfigurable frequency filters, oscillators, and fractional-order elements and active element design.

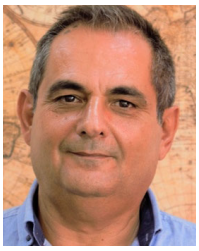

COSTAS PSYCHALINOS (Senior Member, IEEE) received the B.Sc. and Ph.D. degrees in physics and electronics from the University of Patras, Greece, in 1986 and 1991, respectively.

From 1993 to 1995, he worked as a Postdoctoral Researcher with the VLSI Design Laboratory, University of Patras. From 1996 to 2000, he was an Adjunct Lecturer with the Department of Computer Engineering and Informatics, University of Patras. From 2000 to 2004, he served as an Assistant Professor with the Electronics Laboratory, Physics Department, Aristotle University of Thessaloniki, Greece. Since 2004, he has been serving as a Faculty Member of the Electronics Laboratory, Physics Department, University of Patras, where he is currently a Full Professor. His research interests include the development of CMOS analog integrated circuits, including fractional-order circuits and systems, continuous and discrete-time analog filters, amplifiers, and low voltage/low power building blocks for analog signal processing.

Dr. Psychalinos is a member of the Nonlinear Circuits and Systems Technical Committee of the IEEE and CAS Society. He serves as the Editor-in-Chief for the *Circuit and Signal Processing Section of the Electronics* journal (MDPI). He serves as an Area Editor for the *International Journal of Electronics and Communications* (AEU) and an Editor for the *International Journal of Circuit Theory and Applications*. He is currently an Associate Editor of the *Circuits, Systems, and Signal Processing* journal and *Journal of Advanced Research*. He is a member of the Editorial Board of the *Microelectronics Journal*, *Analog Integrated Circuits and Signal Processing*, *Fractal and Fractional*, and *Journal of Low Power Electronics and Applications*.